# Abnormal negative thermal expansion of sodium: A first-principles discovery at high pressures

Shasha Li and Yue Chen*

*Department of Mechanical Engineering, The University of Hong Kong, Pokfulam Road, Hong Kong SAR, China*

(Received 25 May 2017; revised manuscript received 21 September 2017; published 10 October 2017)

Negative thermal expansion coefficients ($\alpha$) are found in the fcc and cI16 (a distorted bcc structure) phases of sodium at pressures above 90 GPa from first principles. At room temperature, the most significant negative $\alpha$ of about $-4.5 \times 10^{-6}$ K$^{-1}$ is predicted in fcc sodium at 120 GPa, which represents the first prediction of a robust negative $\alpha$ in a simple metal. Anharmonic lattice dynamics calculations were carried out to rationalize this intriguing behavior. We find that the negative thermal expansion of fcc sodium originates from the transverse acoustic modes with large negative Grüneisen parameters. Furthermore, full phonon spectra of fcc sodium at elevated temperatures are calculated from perturbation theory. The phonon-phonon couplings in fcc sodium are found to increase abnormally under high pressures.

DOI: 10.1103/PhysRevB.96.134104

## I. INTRODUCTION

Sodium exhibits great complexity under high pressure and has attracted great attention in the last decade. It was found that sodium transforms from the bcc phase to the fcc phase at 65 GPa [1], and then transforms to the cI16 phase—a distorted bcc phase at about 105 GPa [2]. Further compression results in various phases with complex electronic properties [3,4]. It is a metal at ambient pressure, then it transforms to an insulator at 200 GPa with a double hexagonal hP4 structure [4]. It remains as an insulator in a large pressure range of 0.2–15.5 TPa, and then it becomes a metal again at pressures above 15.5 TPa with a cI24 structure [5]. Another interesting feature of sodium is its melting temperature phase diagram. It is found that its melting temperature increases from ambient pressure to 30 GPa, with a melting temperature of about 1000 K at 30 GPa, and then decreases under further compression, with a melting temperature of about 300 K at 120 GPa [6]. In addition to the above intriguing properties, we discover in this paper that sodium has an abnormal negative thermal expansion coefficient under pressure.

Most materials exhibit positive thermal expansion, with expansion coefficients of approximately $1 \times 10^{-5}$, $1 \times 10^{-6}$, and $1 \times 10^{-4}$ K$^{-1}$ for metals, ceramics, and polymers, respectively [7], while materials with negative thermal expansion are relatively rare. Negative thermal expansion was often found in materials with frameworks or networks [8–12], e.g., $ZrW_2O_8$ [8] and some metal-organic framework (MOF) materials [9,10], resulting from the acoustic phonons with low frequencies. It was found that the phonon modes below 50 meV in $ZrW_2O_8$ have negative Grüneisen parameters, leading to its negative thermal expansion [8]; the rigid acoustic phonon modes were found responsible for the negative thermal expansion of MOF structures due to the tilting of their linkers [9,10]. The experimental linear thermal expansion coefficient of sodium at 0 GPa is about $71 \times 10^{-6}$ K$^{-1}$ [13], while its thermal expansion under pressure has never been reported. In the present paper, the thermal expansion of sodium below 150 GPa is studied from first principles. It is found that the fcc and cI16 phases of sodium above 90 GPa exhibit negative thermal expansions.

To better understand the abnormal negative thermal expansion coefficient, Grüneisen dispersion $\gamma$, which represents the effect of changing volume on its vibrational properties, is calculated. In addition, full phonon spectra at elevated temperatures are obtained from perturbation theory and third-order anharmonic force constants. At 0 K, there is no interaction among phonons, thus the phonon lifetime is infinite. At elevated temperatures, the phonon-phonon interactions result in decreased phonon lifetime and frequency shift. Phonon-phonon interactions can be taken into account via the phonon self-energy, $\Sigma_\lambda(\omega) = \Delta_\lambda(\omega) - i\Gamma_\lambda(\omega)$ [14], where the real part $\Delta_\lambda(\omega)$ represents the frequency shift, and $2\Gamma_\lambda(\omega)$ denotes the linewidth of a phonon mode, which is the reciprocal of the phonon lifetime $\tau_\lambda$.

## II. COMPUTATIONAL DETAILS

Density functional theory (DFT) calculations are performed using the Vienna Ab Initio Simulation Package [15]. The valence electronic states of sodium are expanded in plane-wave basis sets with an energy cutoff of 350 eV. The electron-ion interactions are treated with the projector augmented wave method [16] and the exchange-correlation interactions are treated using the generalized gradient approximation of Perdew, Burke, and Ernzerhof [17]. The total energy tolerance is $10^{-8}$ eV. We adopted $6 \times 6 \times 6$ supercells of the bcc and fcc phases and a $3 \times 3 \times 3$ supercell of the cI16 phase, which all contain 216 atoms, to calculate the thermal expansion coefficients. The same supercells were also used to calculate the phonon and Grüneisen dispersions based on the small displacement method using PHONO3PY [18]. Volume changes of $\pm 1\%$ were applied for Grüneisen dispersion calculations. For bcc and fcc phases, Monkhorst pack grids of $4 \times 4 \times 4$ and $3 \times 3 \times 3$ were used for $4 \times 4 \times 4$ and $6 \times 6 \times 6$ supercells, respectively. For the cI16 phase, a Monkhorst pack grid of $3 \times 3 \times 3$ was used for its $3 \times 3 \times 3$ supercell. The width of Gaussian smearing was set to 0.1 eV in our calculation.

## III. RESULTS AND DISCUSSION

The enthalpies of different sodium phases were first calculated to determine the phase transition pressures. The bcc, fcc, and cI16 phases are considered in our calculations based on

*Corresponding author: yuechen@hku.hk

 

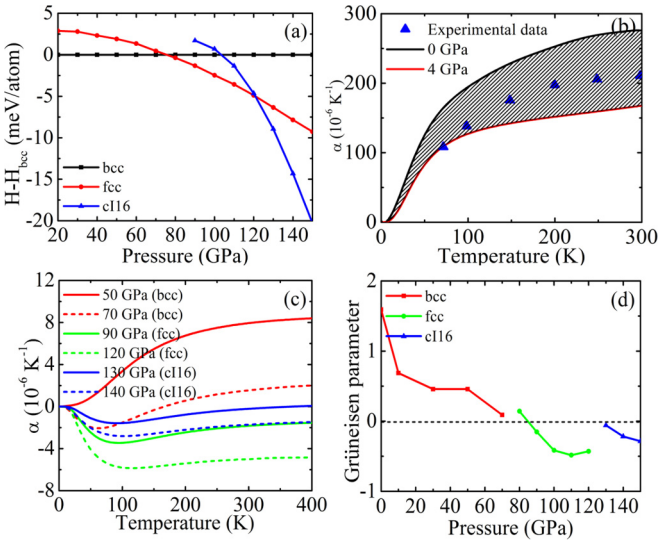


FIG. 1. (a) Enthalpy differences between the competing phases of sodium from 20 to 150 GPa. (b) Thermal expansion coefficient of sodium at ambient pressure. The solid line is obtained from our calculations, and the dots represent experimental measurements [13]. (c) Thermal expansion coefficients of sodium at pressures of 50 GPa (bcc), 70 GPa (bcc), 80 GPa (fcc), 120 GPa (fcc), 130 GPa (cI16), and 140 GPa (cI16). (d) Grüneisen parameters at 300 K as a function of pressure.

previous experimental observations [1,2]. The enthalpy $H$ of a crystal structure under pressure $P$ is defined as $H=U+PV$, where $U$ is the internal energy and $V$ is the volume. It is seen from Fig. 1(a) that the bcc phase transforms to fcc at 80 GPa, and then transforms to cI16 at 130 GPa; our results are consistent with previous theoretical values of 80 [19] and 132 GPa [20], but higher than the experimental values of 65 [1] and 105 GPa [2]. Although our calculations do not precisely reproduce the phase transition pressures, this does not affect the following discussions.

The thermal expansion coefficients of the bcc phase of sodium at 0 and 4 GPa are shown in Fig. 1(b). It is seen that experimental measurements [13] lie within results (see Fig. s1 in Supplemental Material for detailed procedures of thermal expansion coefficient calculations [21]). Although the pressure value does not match exactly with experiments, our thermal expansion calculations are reliable to predict the pressure effects. The structural phase transitions of sodium under high pressures can be correctly reproduced from DFT, although the theoretical transition pressure values may deviate from the experiments. For example, the bcc phase is predicted to transform to fcc at 80 GPa and further transform to cI16 at 130 GPa, whereas the corresponding experimental pressure values are 65 and 105 GPa, respectively. Despite the differences in the exact pressure values, the pressure effects on the phase transitions are successfully captured. Similarly, it is acceptable that the experimental thermal expansion coefficient of sodium at ambient conditions lies in between the theoretical values obtained at 0 and 4 GPa, taking into account the quasiharmonic approximation (QHA). As shown in Fig. 1(c), the thermal expansion coefficient decreases greatly when pressure increases from 0 to 50 GPa, implying significant changes to the lattice anharmonicity. Sodium in the bcc phase below 70 GPa mostly exhibits normal positive thermal expansion, while for fcc sodium negative thermal expansion is predicted to exist in a large temperature range above 90 GPa, i.e., the volume contracts as temperature increases. The absolute value of the thermal expansion coefficient becomes larger as pressure increases, implying that a robust negative thermal expansion coefficient may be achieved. At room temperature, the most robust negative thermal expansion coefficient of $-4.5 \times 10^{-6}$ K$^{-1}$ is found at 120 GPa; this value is comparable to the negative thermal expansion coefficient of $ZrW_2O_8$ ($-9.1 \times 10^{-6}$ K$^{-1}$) [22]. For sodium in the cI16 phase from 130 to 150 GPa, the thermal expansion coefficients are also negative, and the absolute value of the expansion coefficient increases with increasing pressure. It is also found that there are sudden jumps in the thermal expansion coefficient accompanying the phase transitions; the jump is relatively large when sodium transforms from the fcc to the cI16 phase.

The thermal expansion of a crystal is related to the Grüneisen parameter by $\alpha = \frac{\gamma C_p}{VB}$, where $\gamma$ is the Grüneisen parameter, which measures the effect of volume change on the vibrational property and describes the lattice anharmonicity of a crystal; $B$ is the adiabatic bulk modulus; $C_p$ is the constant-pressure heat capacity. Experimentally, the Grüneisen parameters of sodium were measured up to 32 kbars, and it was found that $\gamma$ decreases under compression [23]. In this paper, the Grüneisen parameters at 300 K from 0 to 150 GPa are computed using QHA and fitting thermodynamic parameters with the results given in Fig. 1(d). It is seen that the Grüneisen parameter of sodium in the bcc phase is positive, and it decreases with increasing pressure, which is consistent with experimental observations. The Grüneisen parameter becomes negative when pressure is above 90 GPa for the fcc and cI16 phases of sodium, and the absolute value of $\gamma$ increases with increasing pressure in these two phases, which is abnormal and different from most materials in which the anharmonicity decreases with increasing pressure [23–27]. For example, the Grüneisen parameter of MgO was reported to decrease under pressure using molecular dynamics [25]; the Anderson-Grüneisen parameter of $MgSiO_3$ was found to decrease with increasing pressure using the quasiharmonic approximation combined with first-principles phonon calculations [26]; both the Grüneisen parameter and the Anderson-Grüneisen parameter of bcc iron were found to decrease as pressure increases [27].

The negative Grüneisen parameter accounts for the negative thermal expansion, and the abnormal increase of the absolute value of the Grüneisen parameter at higher pressures results in more negative thermal expansion. Instead of using the Grüneisen parameter to give an overall description of the lattice anharmonicity, the Grüneisen dispersion of individual vibrational modes has been calculated based on phonon dispersions at equilibrium and slightly compressed and expanded volumes. Since the most negative thermal expansion coefficient and Grüneisen parameter are observed in the fcc phase, we mainly focus on fcc sodium in the following discussion.

The Grüneisen parameter of the individual vibrational mode is defined as $\gamma_i = -\frac{V}{w_i}\frac{\partial w_i}{\partial V}$, where $w_i$ is the frequency of a phonon mode and $V$ is the volume. The phonon and Grüneisen

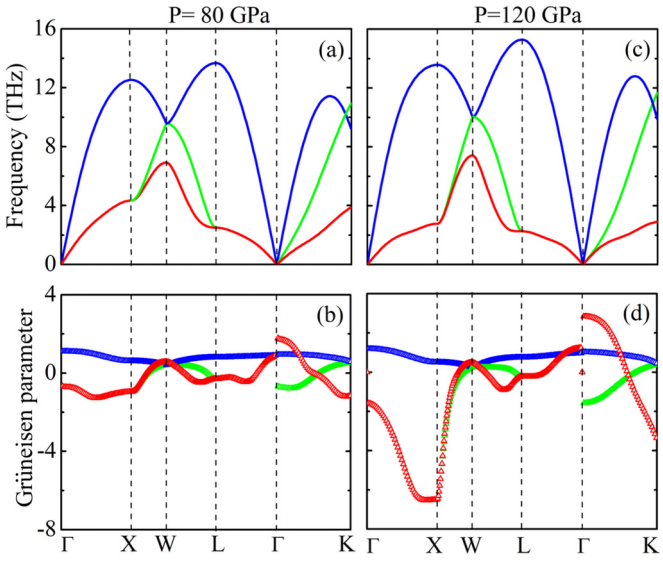


FIG. 2. (a) Phonon dispersions and (b) Grüneisen dispersions of fcc sodium at 80 GPa at 0 K. (c) Phonon dispersions and (d) Grüneisen dispersions of fcc sodium at 120 GPa at 0 K. TA, TA', and LA modes are given in red, green, and blue, respectively.

dispersions of fcc sodium at 80 and 120 GPa are given in Fig. 2. For the Grüneisen dispersions of sodium at 80 GPa, almost all $\gamma_i$ of the longitudinal acoustic (LA) phonons are positive, whereas most of the transverse acoustic (TA) modes exhibit negative $\gamma_i$. The positive thermal expansion coefficient of sodium at 80 GPa is related to the low percentage of phonon modes with negative Grüneisen parameters and the small absolute values of these negative $\gamma_i$. When pressure is increased to 120 GPa, it is found that the Grüneisen parameters of the TA modes along paths Γ-X-W and Γ-K decrease greatly, while the Grüneisen parameters of the TA modes in other paths and those of the TA' and LA modes only have minor changes. As a result, this leads to a negative thermal expansion. Therefore, the negative thermal expansion of fcc sodium under high pressures originates from the TA modes with negative Grüneisen parameters. In addition, Grüneisen dispersions of fcc sodium at 80 and 120 GPa have also been calculated using third-order anharmonic forces (see Fig. s2 in Supplemental Material [21]). It is found that the results obtained from the two methods are in reasonable agreement. The phonon and Grüneisen dispersions of the bcc and cI16 phases of sodium are given in Figs. s3 and s4 in Supplemental Material [21]. For bcc sodium, even though the Grüneisen parameters of the TA modes along path Γ-N become negative as pressure increases from 50 to 70 GPa, the bcc phase at 70 GPa still exhibits positive thermal expansion due to the low percentage of the TA modes with negative Grüneisen parameters. For cI16 sodium, the negative thermal expansion results from the acoustic and optical modes with negative Grüneisen parameters, and the more negative thermal expansion coefficient at higher pressures originates mainly from the acoustic modes with more negative Grüneisen parameters.

The negative thermal expansion of fcc sodium is shown to be related to the anharmonic TA mode. To better understand the lattice dynamics, the vibrational properties at elevated temperatures, i.e., the phonon-phonon coupling effects, need to be further studied. Within harmonic approximation, phonon dispersion is calculated at 0 K, and there is no phonon-phonon interaction. Within quasiharmonic approximation, the anharmonic effect is introduced implicitly by taking into account the volume dependence of temperature, but the phonons are still considered to have infinite lifetimes. In real materials, phonons interact with each other at elevated temperatures and have finite lifetimes; therefore, both the harmonic and quasiharmonic approximations cannot fully describe the vibrational properties at elevated temperatures. To study the phonon-phonon coupling in sodium at finite temperatures, we performed first-principles calculations of the phonon spectra of fcc sodium. Based on the lowest-order perturbation theory, the imaginary part of the self-energy $\Gamma_\lambda(\omega)$ of any phonon mode $\lambda$ can be calculated as follows using PHONO3PY [28]:

$$\Gamma_\lambda(\omega) = \frac{18\pi}{\hbar^2}\sum_{\lambda_1\lambda_2}\left|\Phi_{-\lambda\lambda_1\lambda_2}\right|^2\left\{\left(n_{\lambda_1}+n_{\lambda_2}+1\right)\times\delta\left(\omega-\omega_{\lambda_1}-\omega_{\lambda_2}\right)+\left(n_{\lambda_1}-n_{\lambda_2}\right)\left[\delta\left(\omega+\omega_{\lambda_1}-\omega_{\lambda_2}\right)-\delta\left(\omega-\omega_{\lambda_1}+\omega_{\lambda_2}\right)\right]\right\}, \quad (1)$$

where $\omega_\lambda$ is the harmonic frequency of a phonon mode; $n_i$ is the Bose-Einstein occupation factor,

$$n_i = \frac{1}{\exp(\hbar w_\lambda / k_B T) - 1}; \quad (2)$$

and the matrix $\Phi_{-\lambda\lambda_1\lambda_2}$ represents the interactions among three phonon modes, which can be computed from the third-order anharmonic force constants. Based on the convergency test (see Fig. s5 in Supplemental Material [21]), $6 \times 6 \times 6$ and

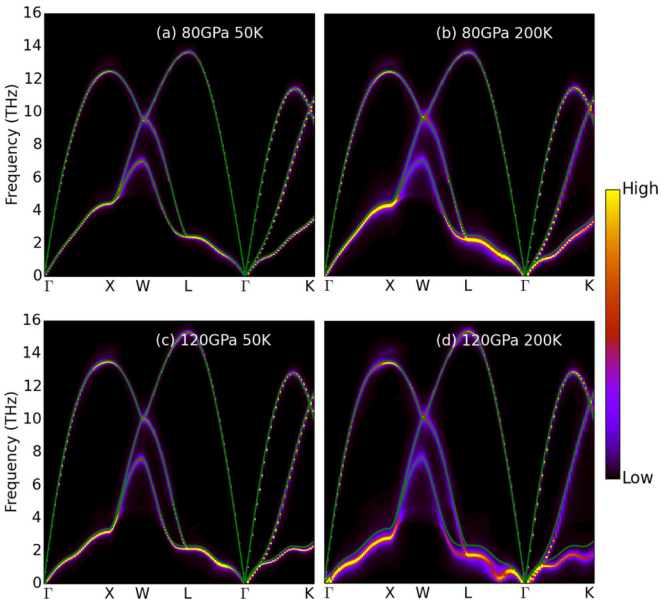


FIG. 3. Phonon spectra of fcc sodium at (a) 50 K and (b) 200 K under a hydrostatic pressure of 80 GPa. Phonon spectra of fcc sodium at (c) 50 K and (d) 200 K under a hydrostatic pressure of 120 GPa are shown. The green curves give the phonon dispersions at 0 K.

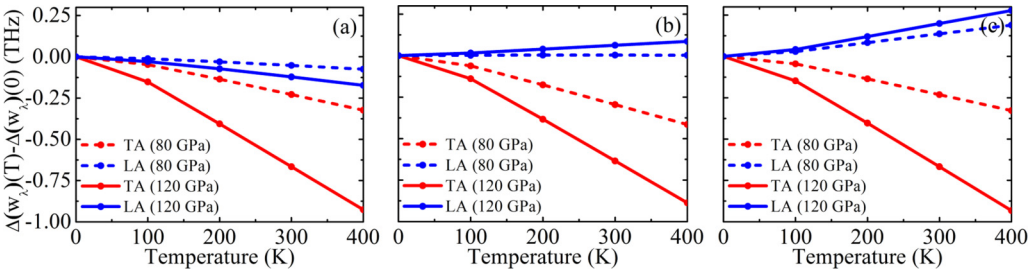


FIG. 4. Temperature-dependent frequency shifts of the TA and the LA phonon modes at the (a) X point, (b) L point, and (c) K point.

$4 \times 4 \times 4$ supercells were used to calculate the second- and third-order force constants of the fcc phase, respectively.

The reciprocal of phonon linewidth $2\Gamma_\lambda(\omega)$ gives the phonon lifetime $\tau_\lambda$:

$$\tau_\lambda = \frac{1}{2\Gamma_\lambda(\omega_\lambda)}. \quad (3)$$

Using the Kramers-Kronig transformation, the real part of self-energy, $\Delta_\lambda(\omega)$, can be calculated:

$$\Delta_\lambda(\omega) = \frac{-2}{\pi} P \int_0^{+\infty} \frac{\omega' \Gamma_\lambda(\omega') d\omega'}{\omega'^2 - \omega^2}, \quad (4)$$

where $P$ is the Cauchy principle value. The power spectrum of a phonon mode can be obtained from [29]

$$\chi''_\lambda(\Omega) \propto \frac{2\omega_\lambda \Gamma_\lambda(\Omega)}{\left[\Omega^2 - \omega_\lambda^2 - 2\omega_\lambda \Delta_\lambda(\Omega)\right]^2 + 4\omega_\lambda^2 \Gamma_\lambda(\Omega)^2}. \quad (5)$$

The phonon spectra of fcc sodium at elevated temperatures under hydrostatic pressures of 80 and 120 GPa are calculated and given in Fig. 3. The solid curves are obtained from harmonic approximation, and represent the phonon dispersions at $T = 0$ K. It is seen that these curves lies on top of the phonon spectra at 0 K. Broadening and softening of the TA modes are observed as temperature increases from 50 to 200 K at both 80 and 120 GPa, indicating stronger phonon-phonon couplings at high temperatures. Interestingly, the temperature effects become more significant with increasing pressure, as evidenced from the more significant broadening and softening of the TA modes at higher pressure, suggesting stronger phonon-phonon couplings as pressure increases. Compared with the significant changes in the TA modes, there are no obvious changes in the LA modes at elevated temperatures under both 80 and 120 GPa. Phonon linewidths originating from electron-phonon interactions have also been investigated, and it is found that the electron-phonon interactions are much weaker than the phonon-phonon interactions (see Fig. s6 in Supplemental Material [21]).

For further examinations of the phonon-phonon couplings in the TA and LA modes, their frequency shifts at X, L, and K points are given in Fig. 4. It is seen that the phonon frequencies of the TA modes shift to lower values as temperature increases, and the shifts become larger under higher pressures. For the LA modes, the phonon frequency decreases with increasing temperature at the X point, while the phonon frequencies increase as temperature increases at L and K points. It is found that the frequency shifts of the TA modes are much larger than those of the LA modes at elevated temperatures, indicating stronger phonon-phonon couplings of the TA modes comparing to the LA modes, consistent with the broadening of the phonon spectra.

## IV. CONCLUSIONS

The thermal expansions of sodium below 150 GPa are studied from first-principles calculations. It is found that fcc and cI16 sodium exhibit abnormal negative thermal expansions above 90 GPa, and the absolute values of the thermal expansion coefficients increase with increasing pressure in these phases. The Grüneisen parameter is investigated to rationalize the negative thermal expansion of fcc sodium. The TA modes with negative Grüneisen parameters are found to contribute to the negative thermal expansion of fcc sodium. By calculating the phonon spectra at finite temperatures using the anharmonic third-order force constants and perturbation theory, we find that the TA modes at low frequencies greatly soften and broaden, exhibiting strong phonon couplings as temperature increases at high pressures.

## ACKNOWLEDGMENTS

We are grateful for financial support from Research Grants Council of Hong Kong under Projects No. 27202516 and No. 17200017, and the research computing facilities offered by Information Technology Services of HKU.

[1] M. Hanfland, I. Loa, and K. Syassen, Phys. Rev. B **65**, 184109 (2002).
[2] M. McMahon, E. Gregoryanz, L. Lundegaard, I. Loa, C. Guillaume, R. Nelmes, A. Kleppe, M. Amboage, H. Wilhelm, and A. Jephcoat, Proc. Natl. Acad. Sci. USA **104**, 17297 (2007).
[3] E. Gregoryanz, L. F. Lundegaard, M. I. McMahon, C. Guillaume, R. J. Nelmes, and M. Mezouar, Science **320**, 1054 (2008).
[4] Y. Ma, M. Eremets, A. R. Oganov, Y. Xie, I. Trojan, S. Medvedev, A. O. Lyakhov, M. Valle, and V. Prakapenka, Nature (London) **458**, 182 (2009).

[5] Y. Li, Y. Wang, C. J. Pickard, R. J. Needs, Y. Wang, and Y. Ma, Phys. Rev. Lett. **114**, 125501 (2015).
[6] E. Gregoryanz, O. Degtyareva, M. Somayazulu, R. J. Hemley, and H.-k. Mao, Phys. Rev. Lett. **94**, 185502 (2005).
[7] O. Guseva, H. R. Lusti, and A. A. Gusev, Modell. Simul. Mater. Sci. Eng. **12**, S101 (2004).
[8] T. R. Ravindran, A. K. Arora, and T. A. Mary, Phys. Rev. Lett. **84**, 3879 (2000).
[9] L. H. Rimmer, M. T. Dove, A. L. Goodwin, and D. C. Palmer, Phys. Chem. Chem. Phys. **16**, 21144 (2014).
[10] S. S. Han and W. A. Goddard, J. Phys. Chem. C **111**, 15185 (2007).
[11] A. Sanson, F. Rocca, G. Dalba, P. Fornasini, R. Grisenti, M. Dapiaggi, and G. Artioli, Phys. Rev. B **73**, 214305 (2006).
[12] T. Chatterji, P. F. Henry, R. Mittal, and S. L. Chaplot, Phys. Rev. B **78**, 134105 (2008).
[13] D. Geldart, R. Taylor, and Y. Varshni, Can. J. Phys. **48**, 183 (1970).
[14] R. Cowley, J. Phys. (Paris) **26**, 659 (1965).
[15] G. Kresse and J. Furthmüller, Comput. Mater. Sci. **6**, 15 (1996).
[16] P. E. Blöchl, Phys. Rev. B **50**, 17953 (1994).
[17] J. P. Perdew, K. Burke, and M. Ernzerhof, Phys. Rev. Lett. **77**, 3865 (1996).
[18] A. Togo and I. Tanaka, Scr. Mater. **108**, 1 (2015).
[19] M. I. Katsnelson, G. V. Sinko, N. A. Smirnov, A. V. Trefilov, and K. Y. Khromov, Phys. Rev. B **61**, 14420 (2000).
[20] H. Eshet, R. Z. Khaliullin, T. D. Kühne, J. Behler, and M. Parrinello, Phys. Rev. Lett. **108**, 115701 (2012).
[21] See Supplemental Material at http://link.aps.org/supplemental/10.1103/PhysRevB.96.134104 for the detailed procedures of thermal expansion coefficient calculations, the Grüneisen dispersion of fcc sodium using the third-order anharmonic force constants, the phonon and Grüneisen dispersion of bcc and cI16 phases using QHA, the convergence test about supercell size used, and the electron-phonon interactions.
[22] G. Barrera, J. Bruno, T. Barron, and N. Allan, J. Phys.: Condens. Matter **17**, R217 (2005).
[23] R. Boehler, Phys. Rev. B **27**, 6754 (1983).
[24] R. J. Hardy, J. Geophys. Res-Sol. EA **85**, 7011 (1980).
[25] I. Inbar and R. Cohen, Geophys. Res. Lett. **22**, 1533 (1995).
[26] B. B. Karki, R. M. Wentzcovitch, S. de Gironcoli, and S. Baroni, Geophys. Res. Lett. **28**, 2699 (2001).
[27] X. Sha and R. E. Cohen, Phys. Rev. B **73**, 104303 (2006).
[28] A. Togo, L. Chaput, and I. Tanaka, Phys. Rev. B **91**, 094306 (2015).
[29] R. Cowley, Rep. Prog. Phys. **31**, 123 (1968).